OPEN ACCESS
IOP Publishing
Classical and Quantum Gravity
Class. Quantum Grav. **41** (2024) 095005 (12pp) https://doi.org/10.1088/1361-6382/ad35a1

Non-stoichiometric silicon nitride for future gravitational wave detectors

G S Wallace[1,7], M Ben Yaala[1,7,*], S C Tait[2], G Vajente[3], T McCanny[4], C Clark[5], D Gibson[6], J Hough[2], I W Martin[2], S Rowan[2] and S Reid[1]

[1] SUPA, Department of Biomedical Engineering, University of Strathclyde, Glasgow, United Kingdom
[2] SUPA, Institute for Gravitational Research, University of Glasgow, Glasgow, United Kingdom
[3] LIGO Laboratory, California Institute of Technology, Pasadena, CA, United States of America
[4] SUPA, Department of Physics, University of Strathclyde, Glasgow, United Kingdom
[5] Helia Photonics Limited, Livingston, United Kingdom
[6] SUPA, School of Computing, Engineering and Physical Sciences, University of the West of Scotland, Paisley, United Kingdom

E-mail: marwa.ben-yaala@strath.ac.uk

Received 20 November 2023; revised 19 February 2024
Accepted for publication 19 March 2024
Published 2 April 2024

Abstract

Silicon nitride thin films were deposited at room temperature employing a custom ion beam deposition (IBD) system. The stoichiometry of these films was tuned by controlling the nitrogen gas flow through the ion source and a process gas ring. A correlation is established between the process parameters, such as ion beam voltage and ion current, and the optical and mechanical properties of the films based on post-deposition heat treatment. The results show that with increasing heat treatment temperature, the mechanical loss of these materials as well as their optical absorption decreases producing films with an extinction coefficient as low as $k = 6.2(\pm 0.5) \times 10^{-7}$ at 1064 nm for samples annealed at 900 °C. This presents the lowest value for IBD SiN_x within the context of gravitational wave detector applications. The mechanical loss of the films

[7] These authors contributed equally to this work.
[*] Author to whom any correspondence should be addressed.

was measured to be $\phi = 2.1(\pm 0.6) \times 10^{-4}$ once annealed post deposition to 900 °C.

Keywords: silicon nitride, gravitational wave detectors, ion beam deposition, thermal noise, optical absorption

1. Introduction

Interferometric gravitational wave detectors (GWDs) rely on highly reflecting mirror coatings with high optical performance (99.999% reflectivity with < 0.5 ppm absorption and < 2 ppm scatter) and low levels of mechanical loss which defines the level of coating Brownian thermal noise (CTN) [1]. At present, the sensitivity of detectors such as Advanced LIGO (aLIGO) are limited by the CTN associated with the alternating layers of titania-doped tantalum pentoxide (TiO_2:Ta_2O_5) as the high index and silica (SiO_2) as the low index materials [2]. With the next iterations of room temperature detectors (e.g. LIGO A+, LIGO A#) aiming to increase their sensitivity by at least a factor 2, new coating materials must be investigated to facilitate this increase in sensitivity.

Silicon nitride (Si_3N_4) has emerged as a promising high index material due to its low mechanical loss both at room temperature [3–6] and cryogenic temperatures [7, 8]. Its high crystallisation temperature [9] also offers the potential to further reduce both mechanical loss and optical absorption, critical factors for enhancing detector sensitivity, while minimising scatter as the coating is still amorphous. Si_3N_4 boasts a refractive index around 2 at 1064 nm [10], giving a suitable index contrast for a GWD HR mirror stack with a low index material such as SiO_2 at both 1064 nm and 1550 nm. However the optical absorption of Si_3N_4 is too high for A+ requirements [11].

The optimisation of the deposition process of SiN*x* has been extensively explored across various methods such as chemical vapor deposition (CVD), plasma enhanced chemical vapor deposition (PECVD), magnetron sputtering, and atomic layer deposition(ALD) [12, 13]. While beam deposition (IBD) offers precise control over film stoichiometry and thickness, as well as dense films with excellent mechanical and electrical properties, it is not commonly used for the fabrication of silicon nitride. This is primarily due to limitations concerning its low deposition rate, complex maintenance, high cost and limited scalability for industrial application. Few studies investigated the impact of different process parameters including the ion beam energy [14–16], deposition temperature [17] and nitrogen partial pressure [18] on the optical and electrical properties of the silicon nitride film however none of these studies focuses on the coatings properties that relevant to GWDs research (i.e mechanical loss and optical absorption).

Non-stoichiometric silicon nitride (SiN_x) has been shown to exhibit low absorption at 1064 nm and 1550 nm while providing an increase in refractive index [8]. This paper presents a systematic study of SiN_x deposited by ion IBD for GWD research. This study uses a custom IBD system to investigate the effects of deposition process parameters, as well as the effects of post deposition heat treatment on the key properties of interest for GWDs.

2. Experimental methods

The SiN_x films were fabricated using the IBD process in a custom-built system presented in figure 1. This process utilises a beam of positively charged particles impingent on a defined surface to eject material from the target and coat adjacent substrates.

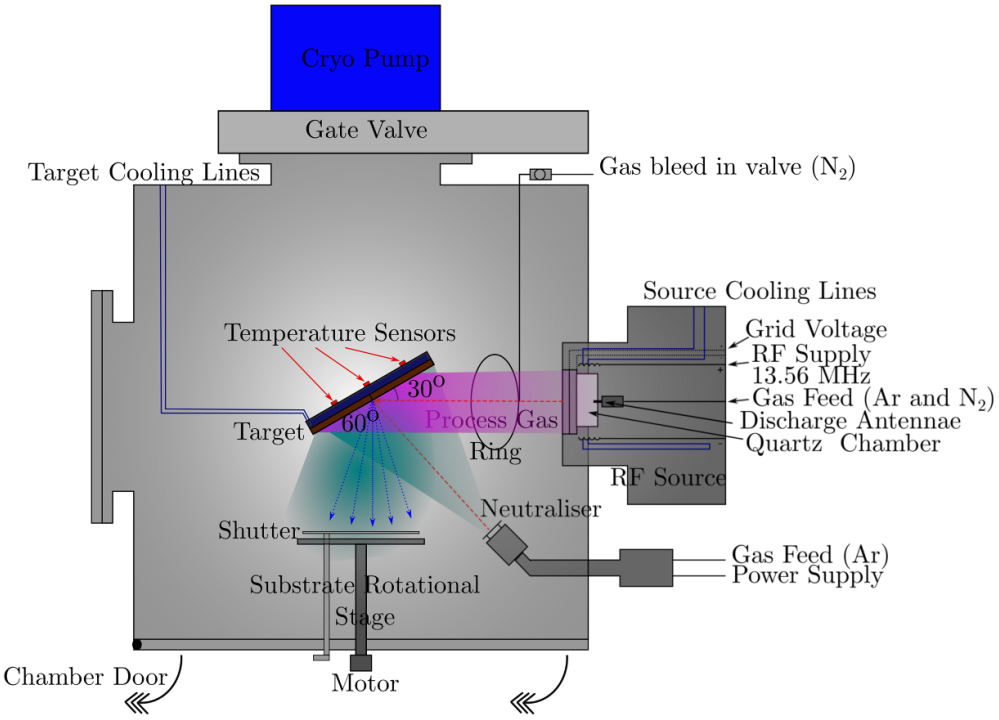

Figure 1. Schematic of radio frequency IBD system utilised in this research. Shown are target and substrate configuration relative to the ion source.

The beam is produced by a 16 cm Veeco radio frequency (RF) ion source [19]. An RF neutraliser is also mounted to ensure no charge build up occurs on surfaces downstream to the plasma. Inside the chamber, a Si target (99.999% purity) is mounted on a custom-built rotating stage that enables the flexibility to mount the target at different angles while maximising film uniformity. Substrates were then mounted on a rotational stage holder that ensures good uniformity across the substrates. All deposition processes here used a fixed target angle (60° relative to the substrates) to maximise the deposition rate [20] and three thermocouples mounted between the stage and target were used to monitor temperature changes during deposition.

Each deposition run included multiple witness substrates consisting of 20 mm diameter 1 mm thick JGS1, JGS3 [21] and 25.4 mm diameter 5 mm thick Corning 7979 fused silica samples for the optical characterisation, 50 mm diameter 0.5 mm thick Corning 7980 fused silica disks for mechanical loss measurements [22], and 20 mm diameter 1 mm thick silicon samples for structural and elemental analysis. Each substrate was cleaned in an ultrasonic bath, using first acetone, then isopropyl alcohol and dried with a N_2 gun prior to coating deposition.

For the deposition process, the vacuum chamber was pumped down to a pressure lower than 1×10^{-6} mbar using a cryopump to remove background water. All deposition runs were performed at room temperature and fixed working gas pressure of 2.4×10^{-4} mbar.

In order to assess the impact of the process parameters on the stoichiometry of the final deposited films, two key parameters of the ion source were varied. The beam current was varied in the range 100 mA–300 mA and the ion energy between 0.4 keV–1.2 keV at 200 mA. The Ar gas flow was fixed to 15 sccm (standard cubic centimeter per minute) and 5 sccm to the ion source and neutraliser respectively. Nitrogen (N_2) was introduced as a sputtering gas

through the RF ion source and/or as a reactive gas in the background using a process gas ring—a circular pipe surrounding the ion beam as shown in figure 1. Both gases are at least 99.998% pure (Grade N4.8). The deposition time was between 1–2 h to avoid target overheating.

The transmittance (T) and reflectance (R) of the deposited coatings were measured between 185–5000 nm using a PhotonRT spectrophotometer (from EssentOptics). The measured values were then implemented in an optical fitting software SCOUT [23] to calculate the refractive index n and the extinction coefficient k. The model here is based on the O'Leary, Johnson, Lim (OJL) model for inter-band transitions [24]. The OJL model has been shown to work well for coatings with high disorder such as the amorphous SiN_x material presented in this study where tail states can exist between the conduction and valence band which decrease exponentially into the band gap [25]. Additionally, an oscillator is used at UV wavelengths (180–300 nm) to simulate O–H bond absorption characteristics that can be incorporated into coatings during the deposition process. To assess the optical absorption characteristics of the SiN_x coatings, photothermal common-path interferometry (PCI) was used [26]. This technique employs a pump-probe setup with two laser beams (high-power, small-diameter pump beam and lower-power, larger-diameter probe beam) intersecting at the material surface. By modulating the pump-beam's intensity at a specific frequency, we directly relate the phase difference in the recovered probe beam to the sample's optical absorption.

To understand their mechanical loss characteristics, the SiN_x films were measured using the gentle nodal suspension (GeNS) method [27–29]. This method measured the free oscillating decay of resonant modes from a 75 mm diameter, 1 mm thick silica disk before and after coating [30]. Both the shift in resonant mode frequency and change in free decay time is dependent on the mechanical properties of the films such as Young's modulus and Poisson ratio. These properties can be used to model the elastic energy distribution in the coated disk, which allows the mechanical loss of the coating to be estimated from the difference in loss before and after coating.

3. Results and analysis

3.1. Molecular nitrogen dissociation for stoichiometric silicon nitride

The silicon nitride thin layers can be produced from a silicon target and N_2 gas in the IBD process either by:

- Dissociation of nitrogen prior to reaching the target surface and the implantation of the atomic nitrogen which is then sputtered bonded or not to silicon by the subsequent ion bombardment from the ion beam.
- Adsorption of molecular nitrogen on the substrate surface (on the forming coating itself) which reacts after with the sputtered Si atoms from the target.

Previous studies [14, 18, 31, 32] showed that the sticking probability of molecular nitrogen on the growing film is negligible due to the high stability of the nitrogen in its molecular form. This suggests that the formation of Si_3N_4 depends on the target nitridation process and on the presence of nitrogen in the process in its reactive (atomic) form.

In this study, the impact of reactive nitrogen flux on film stoichiometry was investigated by introducing nitrogen gas through the RF ion source and the process gas ring. As nitrogen is an inherently unreactive gas this study was to evaluate how the delivery method of nitrogen to the process (either as gas backfilled into the chamber volume or ionised nitrogen from the ion

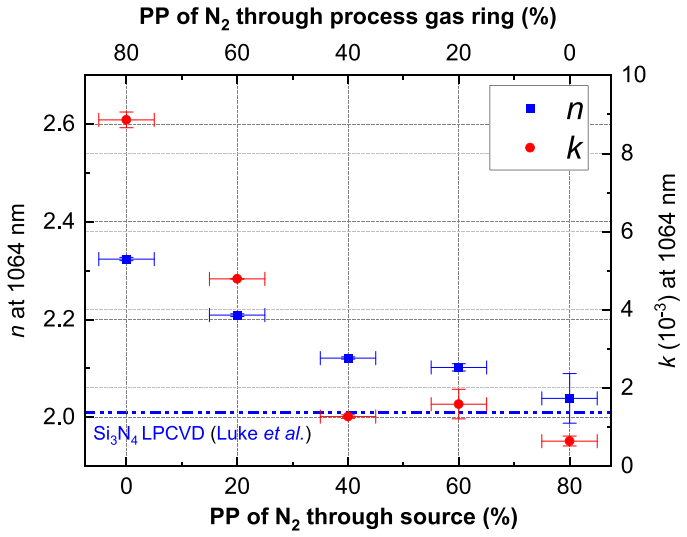

Figure 2. Summary of refractive indices and extinction coefficients for SiN_x coatings with variation of gas partial pressure (PP) through source and process gas ring. Also shown is a reference value of refractive index for stoichiometric Si_3N_4 taken from [33].

source) effects the film composition. The stoichiometry of each film was assessed through direct measurements of the refractive index parameters, n and k, revealing which method is more effective at creating stoichiometric SiN_x coatings while maintaining low optical absorption.

A constant total working pressure was maintained, meaning if more gas was introduced through the source, the partial pressure from the process gas ring was decreased. The idea of using the process gas ring is to inject the gas directly into or the closest possible to the ion beam with the aim of increasing the reactivity of the nitrogen species. With the aim of isolating the effects of the nitrogen gas on these films all deposition runs for this experiment had the same ion source beam parameters (600 keV beam energy, 200 mA beam current). The total gas pressure was also fixed, with the only variation being the percentage of N_2 used expressed in gas partial pressure from the total pressure.

The data in figure 2 shows that by increasing the concentration of N_2 through the ion source, the refractive index is closer to that of Si_3N_4 ($n = 2.04$) in addition to attaining a lower extinction coefficient ($k = 6.43 \times 10^{-4}$). The likely explanation for the process gas ring being less effective in generating coatings with suitable refractive index likely arises from the energy required to break the diatomic bond in N_2. As the bond energy is 9.7 eV for N_2 [34], sufficient energy is needed to break this and create reactive atomic nitrogen. Using the process gas ring to backfill the chamber with gas relies on the energy of Ar ions from the source being sufficient to both break the N_2 molecule efficiently and scatter towards the Si target. This would seem plausible however from the results presented here it can be seen that this method does not create the same quantity of reactive nitrogen as the ion source itself. By discharging the N_2 within the quartz chamber of the ion source as part of the gas feed mixture, the atomic nitrogen created has sufficient kinetic energy to react on the Si target creating SiN_x which is subsequently sputtered towards the substrate to form the final thin film. This is confirmed by the results of figure 3 showing the impact of the ion source parameters including energy and current on the final composition of the coating indirectly expressed by the refractive index.

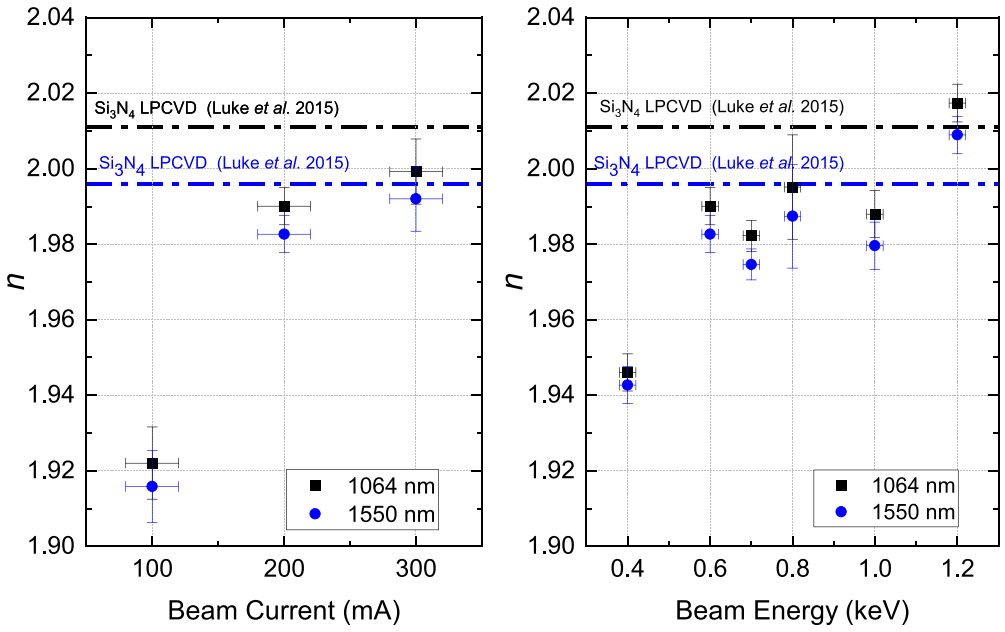

Figure 3. Refractive indices at 1064 nm (black) and 1550 nm (blue) for SiN_x films with varying (left) beam energy (0.4 keV–1.2 keV) at 200 mA current and (right) varying the ion current at fixed beam energy 0.6 keV. Also shown is a reference value of refractive index for stoichiometric Si_3N_4 taken from [33].

The results in figure 3 show an increase in refractive index of the films as both the ion energy and ion current increase. Using higher beam current in an IBD deposition process increases the ion flux of nitrogen atoms impingent on the Si target which at 300 mA reaches the highest refractive index. The beam energy is another factor related to the efficiency of the N_2 dissociation to create reactive nitrogen for the Si_3N_4 formation.

3.2. Optical absorption of SiN_x coatings

Annealing SiN_x coatings has proven to decrease both the optical absorption and the mechanical loss of the deposited thin films [3, 7]. In this study, produced coatings were annealed in air in steps from 500 °C to 900 °C (in 100 °C steps) using a Carbolite Gero 30–3000 C RHF annealing furnace. Each annealing run consisted of a 5 °C min^{-1} ramp in temperature to a set point which the samples were held at for 1 hour before passively cooling (at around 1 °C min^{-1}) to 25 °C. The upper limit of 900 °C was imposed due it being close to the crystallisation temperature of IBD SiO_2 coating ($T_c = 1000$ °C [35]) which would be used in a GWD HR coating design as the low index material.

One key step that needs to be done before studying the optical properties of the films is to check that they are amorphous as deposited and that annealing did not introduce any crystallinity that can induce optical losses through scattering. For that, all coatings were scanned using a Bruker D8 Advance x-ray Diffration (XRD) system. Using both coupled theta and grazing incidence XRD measurements [36], scans were taken between 25° and 60° in order to capture

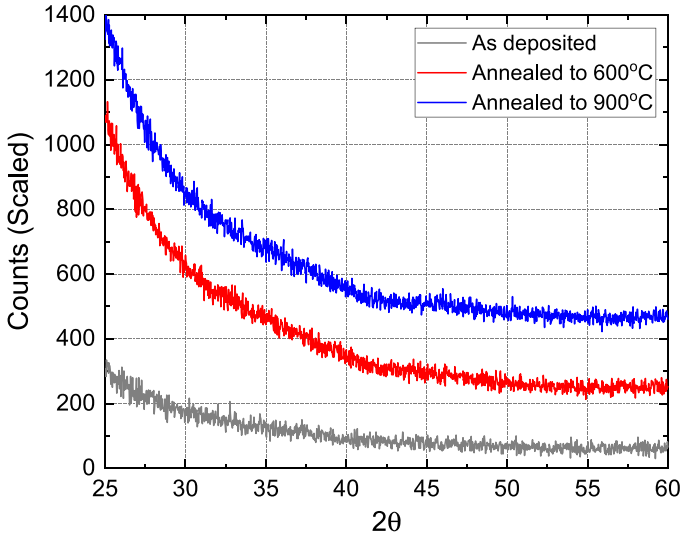

Figure 4. XRD scans for SiN_x coating on SiO_2 at 1.2 keV beam energy and 200 mA beam current. Data is offset on *y*-axis to highlight each scan separately. All scans were done using grazing incidence at an angle of 0.5°.

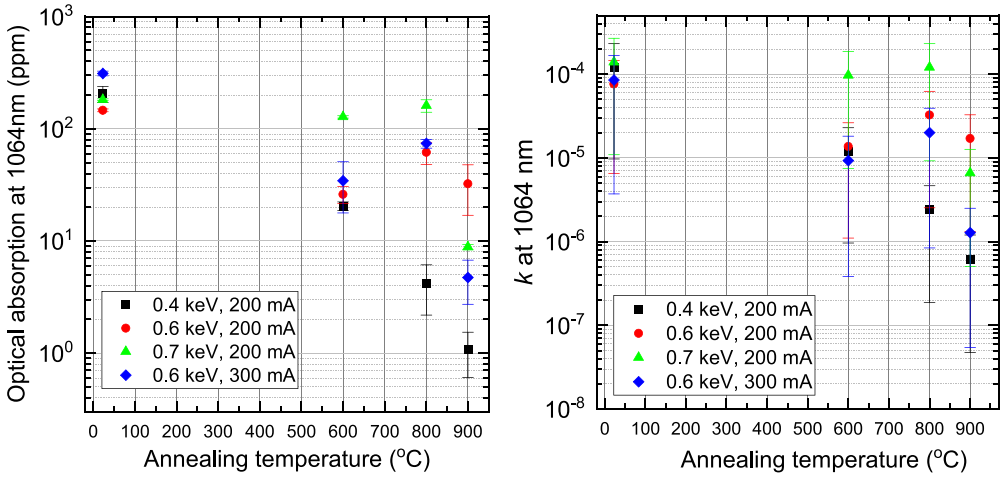

Figure 5. Absorption with coating thickness dependence (left) and calculated extinction coefficient (right) from PCI at 1064 nm with thickness independence for SiN_x samples of varying beam energy and current.

the strong Si_3N_4 crystalline peaks [37, 38]. Figure 4 shows the scan results for SiN_x at 1.2 keV beam energy as deposited and annealed to 600 °C and 900 °C.

Figure 4 show that as deposited and annealed SiN_x samples up to 900 °C have no crystalline sharp peaks and that the samples are fully amorphous. The trailing edge of the scan from 25° to 45° is a result of the JGS grade SiO_2 substrate.

Figure 5 represents the absorption measurement measured by PCI. The *k* values were calculated from the measured PCI absorption (in parts per million (ppm)) to assess the absorption

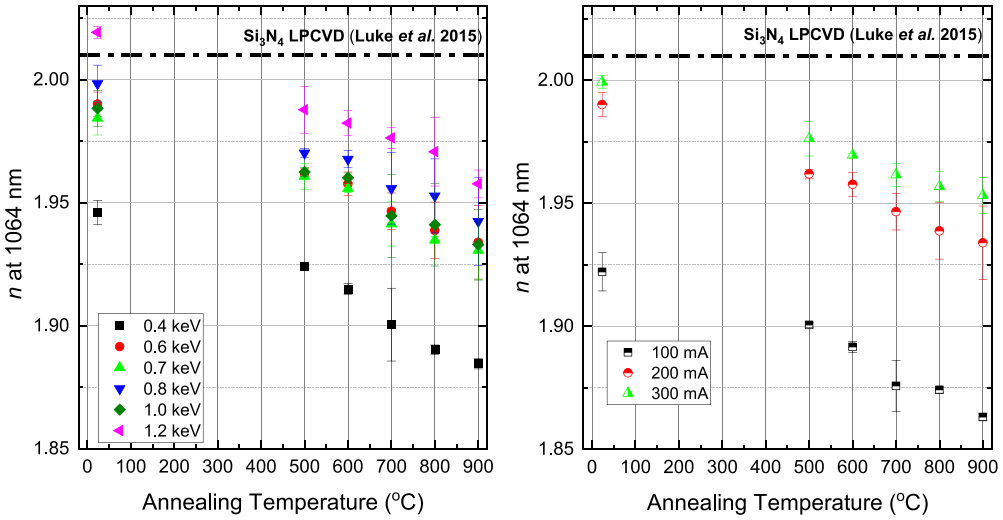

Figure 6. Refractive indices at 1064 nm (black) for SiN_x films with varying beam energy (left) and beam current (right) annealed in steps between 500 °C–900 °C. Also marked is a reference refractive index for LPCVD Si_3N_4 [33]. Error bars are calculated from the R^2 deviation of the plotted R and T spectra.

characteristics of the coatings, irrespective of their thickness. For that, the imaginary component of the materials refractive index is calculated as following:

$$k = \lambda \left(\frac{2\pi t^2 \alpha}{\mathbf{E}\lambda} \right) \frac{1}{4\pi}, \tag{1}$$

where t represents the layer thickness, α the optical absorption and E the electric field intensity. This allows the attenuation of light by the coating material to be expressed through the total absorbed light power and the normalised electric field intensity (**E**) in the layer [39]. The accuracy of the final k produced by this analysis is directly related to how accurately the coating's thickness and refractive index are known.

The results presented in figure 5 show that annealing leads to a reduction in optical absorption, consequently decreasing the extinction coefficient across all samples. The shift in the sequence of ion energies from optical absorption to the k values primarily arises from difference in coating thicknesses (as indicated in equation (1), where k depends on both absorption and thickness). Annealing is shown to reduce the k value of the sample deposited at 300 mA to $1.3(\pm 0.5) \times 10^{-6}$. While low, this value still does not meet the requirement for A+. The lowest value shown is that of the 0.4 keV sample where $k = 6.2(\pm 0.5) \times 10^{-7}$, currently the lowest measured value of k for IBD SiN_x in a GWD application.

Figure 6 shows the calculated refractive index for each temperature step at 1064 nm for the SiN_x films with reference to stoichiometric Si_3N_4. Increasing the ion beam energy resulted in a gradual increase of refractive index in the films towards stoichiometric Si_3N_4. The film with the highest index is that deposited at 1.2 keV where $n = 2.01$ at 1064 nm. Increasing the beam current leads to an increase in refractive indices of the films with 300 mA producing an as deposited index at 1064 nm of $n = 2.00$, very close to stoichiometric Si_3N_4. This suggests that this film is the most stoichiometric film produced which when annealed to 900 °C produced the highest index of all SiN_x films deposited, $n = 1.95$.

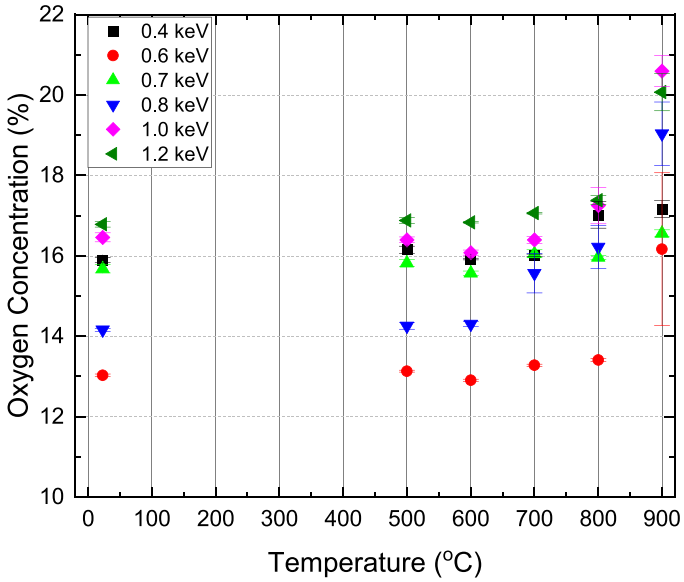

Figure 7. Oxygen concentration in SiN_x coatings produced by varying beam energy (0.4 keV–1.2 keV) as a function of annealing temperature up to 900 °C measured by EDS.

The decrease of the refractive index for annealed coatings can be caused by a structural change of the material and/or an increase of oxygen concentration with annealing. To verify that, the sample's composition was measured by EDS after each annealing step. The results are shown in figure 7. Even in the absence of oxygen being introduced into the vacuum chamber during the procedure, all the coatings manufactured display a significant oxygen content in the range of 13%–17%. This percentage includes the native oxide layer on the surface that forms after exposing the substrate to air (during the transfer from the coating chamber to the EDS measurements), the interstitial O_2 that gets trapped in the coatings in a form of bubble due to the IBD process [40, 41] as well as the dissociated oxygen that gets bonded to the nitrogen and silicon atoms. For fixed beam energy, the oxygen concentration is almost invariable up to 800 °C and increases from 800 °C to 900 °C for all samples suggesting that the refractive index change for temperature below 800 °C is mostly due to the structure change of the silicon (oxy)nitride. It is well know that the IBD method manufactures thin films with high compressive stress. The annealing procedure applied to the SiN_x samples might have relaxed the stress within the film, leading to a reduction in the packing density and consequently causing a decrease in the measured refractive index. Lv *et al* reported similar effect of annealing on the refractive index of ion beam deposited Ta_2O_5 [42]. Further mechanical stress measurements need to be conducted to confirm this.

3.3. Mechanical loss of SiN_x coatings

The study of the mechanical loss of the SiN_x coatings is key to understanding the thermal noise when constructing a HR mirror for a GWD. It has been shown that annealing SiN_x films will reduce the measured mechanical loss [3, 7]. Each coating was measured using the aforementioned GeNS system and annealed after each measurement up to 900 °C. Multiple

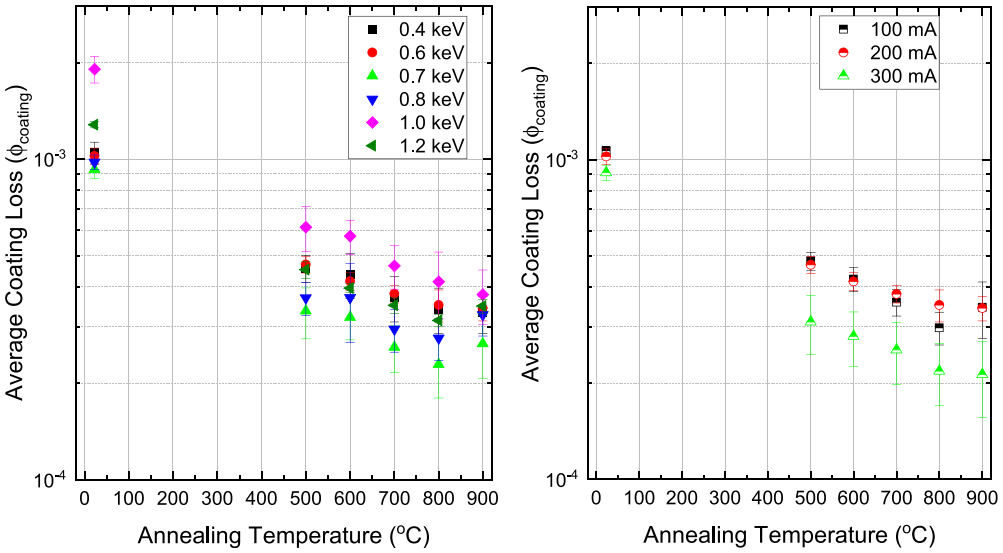

Figure 8. Coating loss of SiN_x annealed up to 900 °C using 0.6 keV beam energy, 100–300 mA current (left) and 0.4–1.2 keV keV beam energy 200 mA current (right) during deposition. Data points are an average of coating loss across multiple resonant modes. Error bars are shown as the standard deviation of measurements.

resonant modes were measured simultaneously up to 32 kHz for each temperature step and averaged to estimate the upper limit of coating loss.

The results presented in figure 8 highlight that increasing the beam current used in the IBD process reduces the mechanical loss of the films produced. Particularly at 300 mA the mechanical loss reduces to $2.1(\pm0.6)\times10^{-4}$ at 900 °C. The increased current density of the beam will result in films with increased packing density which in turn has shown to lead to lower mechanical loss in Si based films [43].

By increasing the beam energy the mechanical loss of the films decreases towards a minimum at 0.7 keV ($\phi = 2.3(\pm0.5)\times10^{-4}$) at 800 °C before increasing at higher energies of deposition. This implies an optimum sputtering energy for Si_3N_4 coordination.

The steep increase in loss for some films at 900 °C is still within the error bars of measurements and can therefore be considered not statistically significant enough to highlight an issue. This is also confirmed by the XRD measurements mentioned previously which show no crystallisation in the films.

4. Conclusion

IBD was utilised to deposit silicon nitride coatings for GWD mirrors application. The fine-tuning of stoichiometry was achieved through manipulation of nitrogen gas flow within the ion source and the utilization of a process gas ring. The ion source demonstrated superior efficiency in achieving the desired stoichiometry by generating highly reactive nitrogen species. The optimisation of the optical and mechanical properties of IBD non-stoichiometric amorphous silicon nitride film was studied by varying the ion source beam energy and current. Additionally, post-deposition thermal annealing was employed to further enhance the optical

and mechanical characteristics of the fabricated coatings, all while preserving their amorphous structure.

The study included a comprehensive analysis of optical absorption across different process parameters. The lowest recorded optical absorption value was observed in the sample deposited with a 0.4 keV beam energy and annealed at 900 °C , where k reached $6.2(\pm 0.5) \times 10^{-7}$ currently standing as the lowest measured k value for IBD SiN_x within the context of GWD applications. Furthermore, the study showed a refractive index decrease with annealing which can be attributed to an increase in oxygen content for annealing temperatures exceeding 800 °C as well as to a stress relaxation during thermal processing for the full temperature range. Additional mechanical stress analysis is required to validate this hypothesis.

The mechanical loss of these films was shown to decrease with increasing beam current. The lowest recorded value in this study was shown to be $\phi = 2.1(\pm 0.6) \times 10^{-4}$ (when deposited using 300 mA beam current with a beam energy of 0.6 keV) and annealed to 900 °C.

Data availability statement

All data that support the findings of this study are included within the article (and any supplementary files).

Acknowledgments

The authors would like to acknowledge that the EDS and XRD work were carried out at the Advanced Materials Research Laboratory (AMRL), at the University of Strathclyde. We are grateful for financial support from STFC (ST/V005642/1, ST/W005778/1, and ST/S001832/1) and the University of Strathclyde. S R is supported by a Royal Society Industry Fellowship (INF/R1/201072). We are grateful to the National Manufacturing Institute for Scotland (NMIS) for support, and we thank our colleagues in the LSC and Virgo collaborations and within SUPA for their interest in this work. This paper has LIGO Document No. LIGO-P2300387.

ORCID iDs

M Ben Yaala https://orcid.org/0000-0002-6754-0875
G Vajente https://orcid.org/0000-0002-7656-6882
I W Martin https://orcid.org/0000-0001-7300-9151

References

[1] Levin Y 1998 *Phys. Rev.* D **57** 659–63
[2] Granata M *et al* 2020 *Class. Quantum Grav.* **37** 095004
[3] Granata M *et al* 2020 *Appl. Opt.* **59** A229
[4] Liu X, Metcalf T H, Wang Q and Photiadis D M 2007 *Proc. Symp. A: Amorphous and Polycrystalline Thin-Film Silicon Science and Technology* vol 989 p 511
[5] Southworth D, Barton R, Verbridge S, Ilic B, Fefferman A, Craighead H G and Parpia J 2009 *Phys. Rev. Lett.* **102** 225503
[6] Amato A *et al* 2018 High-reflection coatings for gravitational-wave detectors: state of the art and future developments *J. Phys.: Conf. Ser.* **957** 012006
[7] Pan H-W, Kuo L-C, Huang S-Y, Wu M-Y, Juang Y-H, Lee C-W, Chen H-C, Wen T T and Chao S 2018 *Phys. Rev.* D **97** 022004

[8] Tsai D-S, Huang Z-L, Chang W-C and Chao S 2022 *Class. Quantum Grav.* **39** 15LT01
[9] Chung Y-K, Kim S-A, Koo J-H, Oh H-C, Chi E-O, Hahn J-H and Park C 2016 *J. Nanosci. Nanotechnol.* **16** 5403–9
[10] Khanna A, Subramanian A Z, Häyrinen M, Selvaraja S, Verheyen P, Thourhout D V, Honkanen S, Lipsanen H and Baets R 2014 *Opt. Express* **22** 5684–92
[11] Steinlechner J, Krüger C, Martin I W, Bell A, Hough J, Kaufer H, Rowan S, Schnabel R and Steinlechner S 2017 *Phys. Rev.* D **96** 022007
[12] Hegedüs N, Balázsi K and Balázsi C 2021 *Materials* **14** 5658
[13] Kaloyeros A E, Pan Y, Goff J and Arkles B 2020 *ECS J. Solid State Sci. Technol.* **9** 063006
[14] Lambrinos M, Valizadeh R and Colligon J 1996 *Appl. Opt.* **35** 3620–6
[15] Huang L, Hipps K, Dickinson J, Mazur U and Wang X 1997 *Thin Solid Films* **299** 104–9
[16] Erler H-J, Reisse G and Weissmantel C 1980 *Thin Solid Films* **65** 233–45
[17] Fourrier A, Bosseboeuf A, Bouchier D B D and Gautherin G G G 1991 *Jpn. J. Appl. Phys.* **30** 1469
[18] Bouchier D, Gautherin G, Schwebel C, Bosseboeuf A, Agius B and Rigo S 1983 *J. Electrochem. Soc.* **130** 638
[19] Veeco Instruments Inc 2002 16cm RF Source Technical Manual (available at: www.veeco.com/products/16cm-high-power-rf-ion-source/)
[20] Bundesmann C and Neumann H 2018 *J. Appl. Phys.* **124** 231102
[21] Optical grade fused quartz (available at: www.universitywafer.com/Wafers_Services/Fused_Silica/fused_silica.html)
[22] Corning hpfs 7979, 7980, 8655 fused silica: optical materials product information (available at: www.corning.com/media/worldwide/csm/documents/HPFS_Product_Brochure_All_Grades_2015_07_21.pdf)
[23] WTheiss Hardware and Software, SCOUT: thin film analysis software (available at: www.wtheiss.com/)
[24] O'Leary S K, Johnson S R and Lim P K 1997 *J. Appl. Phys.* **82** 3334–40
[25] Theiss W The OJL model (available at: www.mtheiss.com/ojlmodel.htm)
[26] Alexandrovski A, Fejer M, Markosian A and Route R 2009 *Solid State Lasers XVIII* **7193** 71930D
[27] Numata K, Bianc G B, Ohishi N, Sekiya A, Otsuka S, Kawabe K, Ando M and Tsubono K 2000 *Phys. Lett.* A **276** 37–46
[28] Cesarini E, Lorenzini M, Cagnoli G and Piergiovanni F 2014 *2014 IEEE Int. Workshop on Metrology for Aerospace, MetroAeroSpace 2014 - Proc.* vol 053904 pp 528–32
[29] Yamamoto K *et al* 2006 *Phys. Rev.* D **74** 022002
[30] Vajente G, Ananyeva A, Billingsley G, Gustafson E, Heptonstall A, Sanchez E and Torrie C 2017 *Rev. Sci. Instrum.* **88** 073901
[31] Edamoto K, Tanaka S, Onchi M and Nishijima M 1986 *Surf. Sci.* **167** 285–96
[32] Yoshinobu J, Ichiro Tanaka S and Nishijima M 1993 *Jpn. J. Appl. Phys.* **32** 1171
[33] Luke K, Okawachi Y, Lamont M R E, Gaeta A L and Lipson M 2015 *Opt. Lett.* **40** 4823–6
[34] Frost D C and McDowell C A 1956 *Proc. R. Soc.* A **236** 278–84
[35] Amato A 2019 Low thermal noise coating for new generation gravitational-wave detectors *PhD Thesis* Université de Lyon
[36] Simeone D, Baldinozzi G, Gosset D, Le Caer S and Bérar J-F 2013 *Thin Solid Films* **530** 9–13
[37] Abbas K, Ahmad R, Khan I, Ikhlaq U, Saleem S and Ahson R 2013 Role of argon plasma on the structural and morphological properties of silicon nitride films by pulsed DC glow discharge *2013 Int. Conf. on Aerospace Science & Engineering (ICASE)* (IEEE) pp 1–5
[38] Schmidt H, Gruber W, Borchardt G, Bruns M, Rudolphi M and Baumann H 2004 *Thin Solid Films* **450** 346–51
[39] Arnon O and Baumeister P 1980 *Appl. Opt.* **19** 1853–5
[40] Gier C *et al* 2023 *Thin Solid Films* **771** 139781
[41] Harthcock C *et al* 2019 *Appl. Phys. Lett.* **115** 251902
[42] Lv Q, Huang M, Zhang S, Deng S, Gong F, Wang F, Pan Y, Li G and Jin Y 2018 *Coatings* **8** 150
[43] Jacks H C 2018 *Identifying Structures Responsible for Two-Level Systems in Amorphous Silicon* (University of California)